Chinese Physics C Vol. 39, No. 5 (2015) 057002

Effect of the transverse parasitic mode on beam performance for the ADS driver linac in China

CHENG Peng(程鹏)[1] PEI Shi-Lun(裴士伦) WANG Jiu-Qing(王九庆) LI Zhi-Hui(李智慧)

Institute of High Energy Physics, Chinese Academy of Sciences, Beijing 100049, China

Abstract: The ADS (Accelerator Driven subcritical System) driver linac in China is designed to run in CW (Continuous Wave) mode with 10 mA designed beam current. In this scenario, the beam-induced parasitic modes in the ADS driver linac may make the beam unstable or deteriorate the beam performance. To evaluate the parasitic mode effect on the beam dynamics systematically, simulation studies using the ROOT-based numerical code SMD have been conducted. The longitudinal beam instability induced by the HOMs (High Order Modes) and SOMs (Same Order Modes) has little effect on the longitudinal beam performance for the current ADS driver linac design based on the 10 MeV/325 MHz injector I from previous studies. Here the transverse parasitic mode (i.e., dipole HOM) effect on the transverse beam performance at the ADS driver linac exit is investigated. To more reasonably quantify the dipole mode effect, the multi-bunch effective emittance is introduced in this paper.

Key words: parasitic mode, dipole mode, HOM, beam dynamics, beam instability

PACS: 29.27.Bd **DOI:** 10.1088/1674-1137/39/5/057002

1 Introduction

Figure 1 shows the general layout of the ADS (Accelerator Driven subcritical System) driver linac in China, which is designed to run in CW (Continuous Wave) mode with 10 mA designed beam current [1]. Two families of superconducting elliptical 5-cell cavities with β=0.63 and β=0.82 are used to boost the proton beam energy from 180 MeV to 1.5 GeV.

When the particle beam travels through the RF (Radio Frequency) cavity, the parasitic modes will be excited. Longitudinal monopole High Order Modes (HOMs) and Same Order Modes (SOMs) can be excited wherever the beam goes on-axis or off-axis, and will affect the beam energy and energy spread. Transverse dipole HOMs can only be excited by the off-axis beams, and will dilute the transverse beam quality.

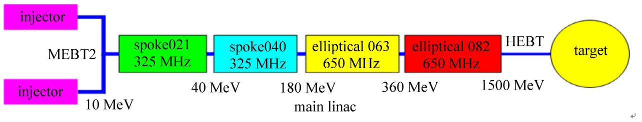

Fig. 1. General layout of the ADS driver linac.

For the lower energy part of the ADS driver linac, due to the relatively high beam intensity (10 mA nominal beam current), the space charge effect plays the most important role for the beam performance dilution. Therefore, only the higher energy superconducting section from 180 MeV to 1.5 GeV is considered in the parasitic mode effect studies, and the parasitic mode characteristics dependence on the particle beam velocity are also considered. It has been shown in Ref. [2] that the longitudinal beam instability induced by the HOMs and SOMs has little effect on the longitudinal beam performance for the current ADS driver linac design based on the 10 MeV/325 MHz injector I. In this paper, the transverse parasitic mode (i.e. dipole HOM) effect on the transverse beam performance at the ADS driver linac exit is investigated by using the ROOT-based numerical code SMD [3].

Due to the unavoidable existence of the parasitic modes and the various randomly distributed jitter and error effects within the tolerable limits, the transverse beam quality of each bunch at the ADS driver linac exit cannot be completely the same as the others. From the beam dynamics design point of view, the beam transport line downstream of the ADS driver linac should have the capability to successfully transport all the bunches in the CW bunch train to bombard the target to produce neutrons. In this situation, the reasonable way to quantify the parasitic mode effect on the transverse beam quality at the ADS driver linac exit is to evaluate the multi-bunch emittance. Thus, in the studies conducted in this paper, the multi-bunch effective emittance is introduced. Finally, based on a large amount of numerical simulat-

---

Received 14 July 2014, Revised 3 November 2014

[1] E-mail: chengp@ihep.ac.cn

ions, some conclusions concerning the transverse parasitic mode effect have been made.

2 Basic theory

When a particle with charge q travels through the RF cavity off-axis, the excited dipole mode voltage can be given by

$$\Delta V_{\perp,n}=\frac{1}{2}\mathrm{i}xq\frac{\omega_n^2}{c}\left(\frac{R}{Q}\right)_{\perp,n}(\beta), \tag{1}$$

where ω_n is the angular frequency of the specific dipole mode n, x is the particle's transverse location relative to the cavity axis, β is the particle's normalized velocity, i means the particle induced voltage is 90° out of phase with the particle, hence there is no direct action between the voltage and the particle itself. $(R/Q)_{\perp,n}$ is defined as

$$\left(\frac{R}{Q}\right)_{\perp,n}(\beta)=\frac{\left|\mathrm{i}\left(\frac{c}{\omega_n r_0}\right)\int_{-\infty}^{\infty}E_{z,n}(r=r_0,z)\mathrm{e}^{\mathrm{i}\omega_n(z/\beta c)}\mathrm{d}z\right|}{\omega_n U_n}, \tag{2}$$

where U_n is the stored energy, $E_{z,n}(r=r_0,z)$ is the electric field component along a straight line at the position $r=r_0$ parallel to the cavity axis. As time evolves, the dipole mode voltage will decay exponentially due to the cavity wall power dissipation,

$$V_{\perp,n}(t)=\Delta V_{\perp,n}\mathrm{e}^{-t/T_{\mathrm{d},n}}\mathrm{e}^{\mathrm{i}\omega_n t}, \tag{3}$$

where $T_{\mathrm{d},n}=2Q_{\mathrm{L},n}/\omega_n$ is the decay time constant. Here, $Q_{\mathrm{L},n}$ is the loaded quality factor with the definition of

$$\frac{1}{Q_{\mathrm{L},n}}=\frac{1}{Q_{0,n}}+\frac{1}{Q_{\mathrm{ext},n}}. \tag{4}$$

$Q_{0,n}$ and $Q_{\mathrm{ext},n}$ are the unloaded and external quality factors of mode n, respectively. For the superconducting RF cavity, $Q_{0,n}$ is at the order of 10^{10}, which is much higher than $Q_{\mathrm{ext},n}$, therefore $Q_{\mathrm{L},n}$ is approximately equal to $Q_{\mathrm{ext},n}$.

The dipole mode n excited by the head particles in a bunch, or the upstream bunches in a bunch train, will act on the tail particles or the downstream bunches. According to the Panofski-Wenzel theorem [4], the resulting transverse momentum kick by the dipole mode voltage $V_{\perp,n}$ can be represented by

$$\Delta p_{\perp,n}=q\frac{R(V_{\perp,n})}{c}, \tag{5}$$

which gives a change of the transverse trajectory inclination for an angle of

$$\Delta x'=\frac{\Delta p_{\perp,n}}{p_{\parallel}}=q\frac{R(V_{\perp,n})}{cp_{\parallel}}, \tag{6}$$

where $p_{\parallel}$ is the longitudinal momentum, and $R(V_{\perp,n})$ is the imaginary part of the dipole mode voltage.

For a bunch train consisting of more than one bunch, the induced dipole mode voltages should be summed up, and their phase relationship and exponential decay should also be considered.

3 Simulation execution

3.1 Methodology

The transverse plane logical module of the numerical code SMD is used in the transverse parasitic mode effect simulation studies. Due to the ROOT-based characteristic, SMD has very fast simulation speed and powerful mass output data dealing capability.

The drift-kick-drift model [5] is used to model the beam and cavity interaction. At the mid-plane of each cavity, the particle will interact with the cavity. Therefore, the linac can be modeled as a series of drifts and kicks. Point-like bunches are tracked through each linac, i.e., only the multi-bunch instead of the single bunch effect is studied. The transverse displacement and trajectory inclination angle of each point bunch at the linac exit can be finally obtained. The 2×2 transfer matrices extracted from the multi-particle tracking code TraceWin [6] are used to model the transverse beam dynamics between the mid-planes of the neighbouring two cavities.

To boost the proton beam energy from 180 MeV to 1.5 GeV for the ADS driver linac, ∼14 lattice periods with β=0.63 and ∼20 lattice periods with β=0.82 are planned, the architectures of which are shown in Fig. 2.

Due to the CW mode operation, ∼6500 k point-like proton bunches are launched at the β=0.63 section entrance to let the simulation result reach a steady state. At the β=0.82 section exit, the transverse displacement and trajectory inclination angle of each point-like bunch will be recorded.

3.2 Multi-bunch effective emittance

In SMD, the transverse emittance of the point-like bunches are defined as

$$\begin{aligned}\varepsilon_r&=\pi\sqrt{\left(\frac{1}{N}\sum_1^N(x_i^2)\right)\cdot\left(\frac{1}{N}\sum_1^N(x_i'^2)\right)-\left(\frac{1}{N}\sum_1^N(x_i\cdot x_i')\right)^2}\\&=\pi\sqrt{\langle x^2\rangle\langle x'^2\rangle-\langle xx'\rangle^2}\end{aligned} \tag{7}$$

where x is the transverse displacement, x' is the trajectory inclination angle and N is the bunch total number.

For a proton linac running in pulsed mode with a relatively low duty factor (e.g., 5% for SPL [5], 4% for ESS [7] and 6% for SNS [8], etc), Eq. (7) and $\varepsilon_{\mathrm{HOM}}/\varepsilon_r$ ($\varepsilon_{\mathrm{HOM}}$ and ε_r for the transverse emittance with and without the dipole mode impact respectively) are usually used to evaluate the dipole mode induced beam emittance deterioration. By using Eq. (7), the emittance increase against the duty factor for SPL is simulated and shown in Fig. 3. At 50 Hz repetition rate, the duty factor is varied from 5% to 100% by changing the macro pulse length. Except $Q_{\text{ext}}=1\times10^8$ and $I_{\text{beam}}=400$ mA, the other parameter settings are completely the same as those listed in Ref. [5]. It can be seen that the dipole mode emittance increase for the designed 5% duty factor is only 8%, which is not a big number and indicates that the dipole mode effect can be roughly neglected for the pulsed machine with a relatively low duty factor.

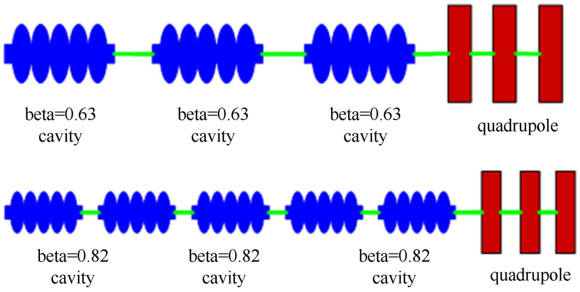

Fig. 2. Architecture for each lattice period of the β=0.63 and β=0.82 superconducting sections.

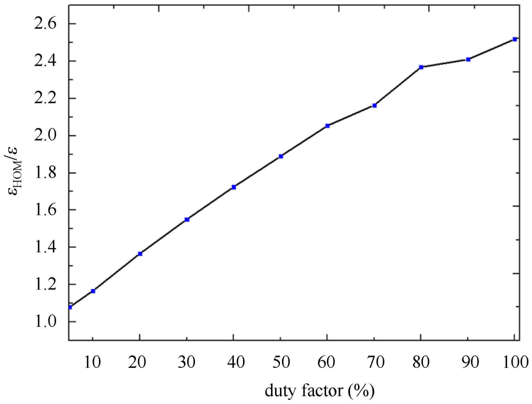

Fig. 3. Emittance increase at the SPL linac exit when the duty factor is varied at a repetition rate of 50 Hz.

The reason for the relatively low emittance growth at low duty factor is that the beam induced dipole mode voltage can be sufficiently decayed to a safety level before the next macro beam pulse comes. As the duty factor increases, due to the non-sufficient decay of the dipole mode voltage, the resulting ε_{HOM} will reach several times that of ε_r, especially for the CW case with 100% duty factor. In this scenario, by using Eq. (7) and $\varepsilon_{\text{HOM}}/\varepsilon_r$, it seems at first glance that the dipole mode effect is very severe, while the truth may be the opposite. To reflect the real situation, it is more reasonable to use the multi-bunch effective emittance and the corresponding emittance increase.

By using the (ξ, η) transformation, the conventional elliptical phase space defined by the coordinates (x, x') can be translated to a circular one as shown in Fig. 4. The new coordinates (ξ, η) are defined as

$$\xi=\frac{x}{\sqrt{\beta}},\quad \eta=\frac{\alpha x+\beta x'}{\sqrt{\beta}}, \tag{8}$$

where α and β are the Twiss parameters. With the single bunch emittance $\varepsilon_0=\pi r_0^2$ and the muti-bunch center dilution $\varepsilon_r=\pi r^2$ (same value as Eq. (7)), the multi-bunch effective emittance and the corresponding emittance increase can be expressed as $\varepsilon_R=\pi(r+r_0)^2$ and $\varepsilon_R/\varepsilon_0=\left(1+\sqrt{\varepsilon_r/\varepsilon_0}\right)^2=(1+r/r_0)^2$, respectively.

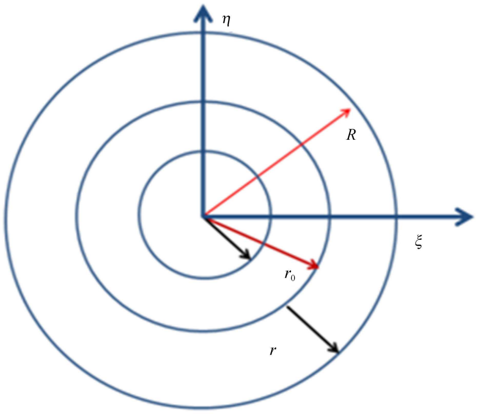

Fig. 4. The circular phase space represented by the coordinates (ξ, η).

3.3 Simulation result

For the ADS driver linac, the single bunch emittance ε_0 at the linac exit is 0.26 πmm·mrad for the 10 mA nominal beam [2]. By applying the beam input parameters listed in Table 1 at the β=0.63 section entrance, at the linac exit the SMD simulated multi-bunch center dilution ε_r without the dipole mode effect is 0.023 πmm·mrad, which has no dependence on the simulated beam current. Then the corresponding multi-bunch effective emittance and the emittance increase are ε_R=0.44πmm·mrad and $\varepsilon_R/\varepsilon_0=\left(1+\sqrt{\varepsilon_r/\varepsilon_0}\right)^2$=1.68, respectively.

Table 1. Beam input parameters with jitter effects.

parameter	value	σ
input energy/MeV	180	0.078
phase/(°)	–25∼–12	0.4
beam current/mA	100	3%
x/mm	0.0	0.3
x'/mrad	0.0	0.3

When the dipole mode effect is considered, the SMD simulated multi-bunch effective emittance increase $\varepsilon_{R,\text{HOM}}/\varepsilon_0$ at the linac exit results from both the beam input jitters and the dipole modes. Here, $\varepsilon_{R,\text{HOM}}/\ \varepsilon_R$ can be used to quantify the emittance increase induced only by the dipole mode, while $\varepsilon_R/\varepsilon_0-1=68\%$ for the corresponding tolerable limit of the emittance increase rate. In this situation, the tolerable limit of $\varepsilon_{R,\mathrm{HOM}}/\varepsilon_0$ and $\varepsilon_{R,\mathrm{HOM}}/\varepsilon_R$ would be 1+68%+68%=2.36 and (1+68%+68%)/(1+68%)=1.40, respectively.

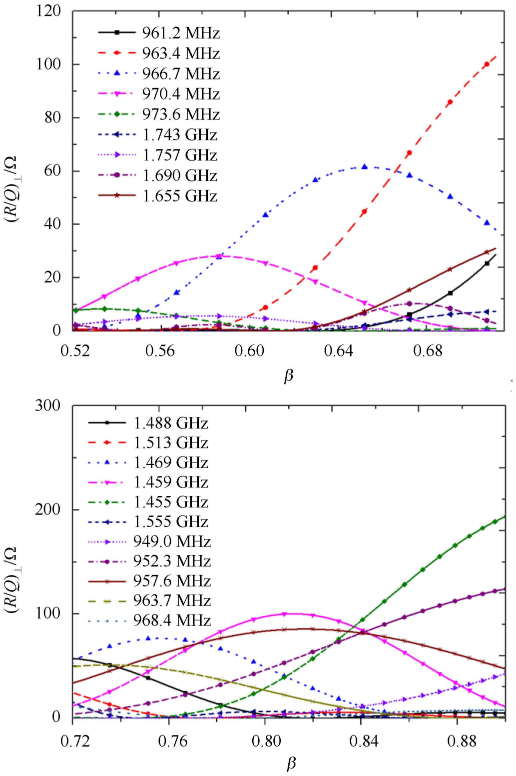

Fig. 5. $(R/Q)_\perp$ dependence on the particle velocity for the dipole modes in the β=0.63 and β=0.82 sections.

It should be pointed out that SMD only calculates the multi-bunch center dilution ε_r and $\varepsilon_{r,\mathrm{HOM}}$, therefore $\varepsilon_{R,\mathrm{HOM}}$ and $\varepsilon_{R,\mathrm{HOM}}/\varepsilon_R$ depend on ε_0. However, since only the ε_0 at the 10 mA nominal current is known at present and the simulation for the cases at higher beam currents (e.g., 100 mA) is used as a safety margin to evaluate the multi-bunch parasitic mode effect, the same ε_0=0.26 πmm·mrad is used in all the following contexts for the beam current ranging from 10 mA to 100 mA.

3.3.1 Effect of HOMs from CST MWS simulation

The dipole mode characteristics for the 5-cell elliptical cavities in the β=0.63 and β=0.82 sections are calculated by using CST MWS (Microwave Studio) [9] and shown in Fig. 5. The modes resonating at 966.7 MHz for the β=0.63 section and 1459 MHz for the β=0.82 section have the highest overall $(R/Q)_\perp$ in the corresponding linac section, and are used as default in the simulation by including the $(R/Q)_\perp$ dependence on the particle beam velocity. A Gaussian RMS frequency spread of 1 MHz is used for all modes [2].

In order to statistically estimate the dipole mode effect, 100 linacs are simulated with a different seed generator for each kind of parameter setup. Finally the averaged emittance increase can be obtained.

Figure 6 shows the averaged multi-bunch effective emittance increase against the damping factor Q_{ext} by considering only the beam input jitters listed in Table 1. The beam current I_{beam} varies from the nominal value of 10 mA to a maximum of 100 mA for the safety margin consideration. No significant emittance increase for the 10 mA beam with $Q_{\mathrm{ext}}=10^8$, and no HOM coupler is needed at this situation. Even at the safety margin beam current of 100 mA with $Q_{\mathrm{ext}}=10^8$, $\varepsilon_{R,\mathrm{HOM}}/\varepsilon_R$ is only 1.17 which is smaller than the tolerable limit 1.4.

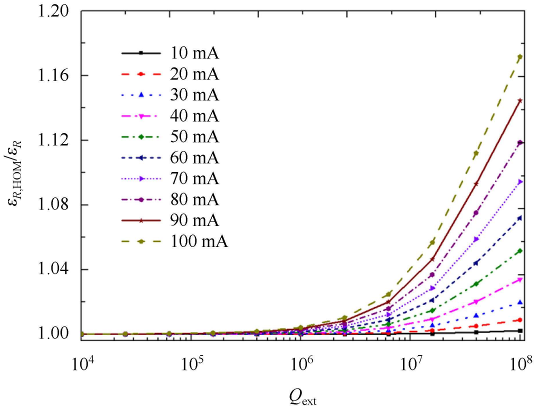

Fig. 6. Multi-bunch effective emittance increase against the damping Q_{ext} for different beam current I_{b}.

To investigate the dependence of initial beam position and trajectory tilt jitter, Fig. 7 shows the averaged multi-bunch effective emittance against the initial RMS transverse beam position jitter and trajectory tilt jitter at a relationship of σ_x/σ'_x=1 mm/1 mrad. The damping Q_{ext} is set to 10^8. The case without considering the dipole mode effect is also shown by setting the simulated beam current to 0 mA. As one can see, the multi-bunch effective emittance at the linac exit, which is smaller than the tolerable limit 0.61πmm·mrad obtained from Eq. (9), is linearly proportional to the initial transverse beam position jitter σ_x and trajectory tilt jitter σ'_x.

The dipole modes can also be excited by the cavity misalignment and off-axis injected beam, both of which will strengthen the dipole mode effect only induced by the beam input jitters, therefore it is necessary to investigate the further deterioration of the beam quality caused by the off-axis injected beam at the β=0.63 section entrance and the cavity misalignment along the β=0.63 and β=0.82 sections.

The cavity misalignment has a Gaussian distribution with a deviation of $\sigma_{\mathrm{d}x}$, which is varied from 0.1 mm to 10 mm. 100 linacs are simulated for each $\sigma_{\mathrm{d}x}$ at $I_{\mathrm{beam}}=$

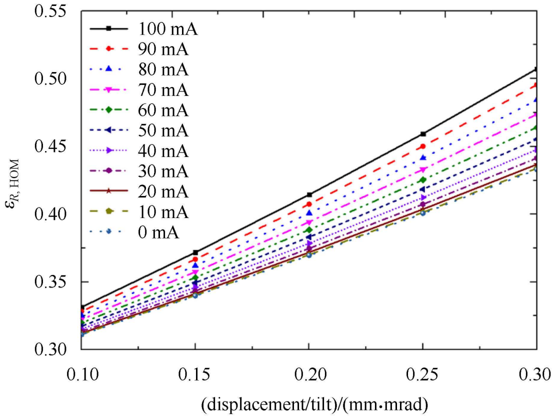

Fig. 7. Multi-bunch effective emittance against the initial RMS transverse beam position jitter σ_x and trajectory tilt jitter σ'_x for different I_{beam}.

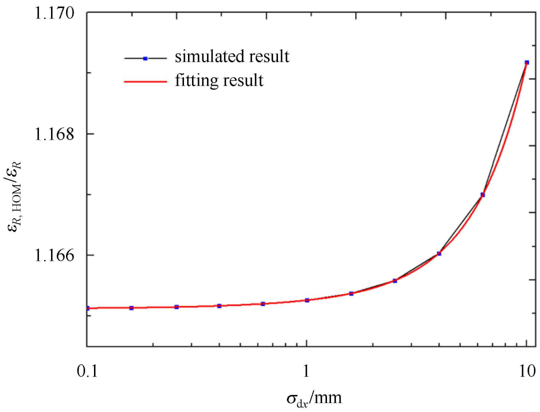

Fig. 8. Multi-bunch effective emittance increase against cavity misalignment $\sigma_{\mathrm{d}x}$.

100 mA. All other parameters are default ones. Fig. 8 shows the multi-bunch emittance increase at the ADS driver linac exit as a function of $\sigma_{\mathrm{d}x}$. The emittance increase caused only by the cavity misalignment is proportional to $\sigma_{\mathrm{d}x}^2$ and starts to rise rapidly above $\sigma_{\mathrm{d}x}$=1 mm. Since the expected $\sigma_{\mathrm{d}x}$ for the ADS driver linac in China is in the order of 1 mm, the dipole mode effect induced by the cavity misalignment can be neglected. Fig. 9 shows the multi-bunch emittance increase when the 100 mA proton beam is injected off-axis at the β=0.63 section entrance. The transverse injected beam position is varied from −10 mm to +10 mm. Since the multi-bunch centre dilution defined in Eq. (7) is not translation invariant and a mean off-axis injection position leads to an increase of ε_r, the following translation invariant formula [5] is defined,

$$\varepsilon^{*}=\pi\sqrt{\langle x^2\rangle\langle x'^2\rangle-\langle xx'\rangle^2-2\bar{x}\cdot\bar{x}'+\bar{x}'^2\langle x^2\rangle+\bar{x}^2\langle x'^2\rangle}, \quad (9)$$

where $\bar{x}$ and $\bar{x}'$ are the mean values of the transverse injection position and the tilt distribution. The additional emittance increase caused by the off-axis injection is only ~1.7% for −10 mm offset, while it is ~3.1% for +10 mm offset.

3.3.2 Effect of HOMs sitting on the machine line

The most dangerous situation is the HOMs sitting on the machine line, the frequency of which is a multiple of the bunch frequency. To evaluate this kind of HOM effect, the simulation has been done by setting the dipole mode frequency to 1300 MHz (4 times the bunch frequency) in both the β=0.63 and β=0.82 sections. Default parameters listed in Table 3 have been used. In reality, the probability of the beam induced dipole mode sitting on the machine line is relatively low, therefore the $(R/Q)_{\perp}$ is set to be 10 Ω.

For 1 MHz RMS frequency spread width, Fig. 10 shows the corresponding emittance increase against the simulated beam current ranging from 10 mA to 100 mA. Q_{ext} is set to 108.

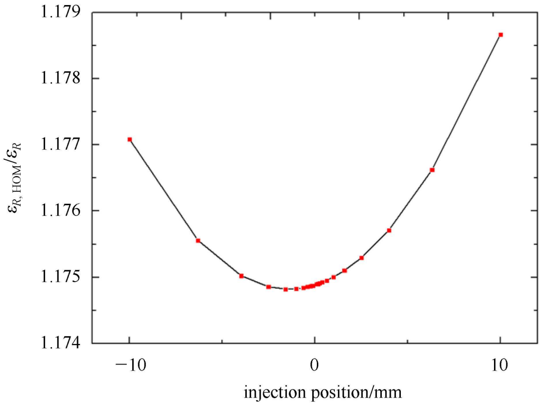

Fig. 9. Multi-bunch emittance increase against transverse beam injected position.

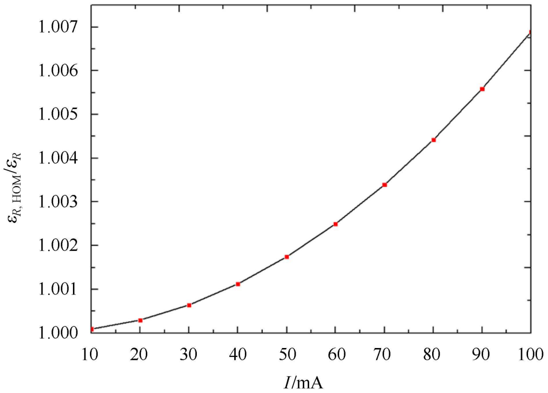

Fig. 10. Multi-bunch emittance increase against beam current which is varied from 10 mA to 100 mA.

Figure 11 shows the emittance increase against the RMS frequency spread width ranging from 100 kHz to 1 MHz. The simulated beam current is 100 mA and Q_{ext}=108. Even for 100 kHz frequency spread width, the emittance increase rate caused by the dipole mode sitting on the machine line is only 0.76%, which can be completely ignored. However, the HOM frequency spread width in reality is usually at the level of 1 MHz [6], which is fairly large.

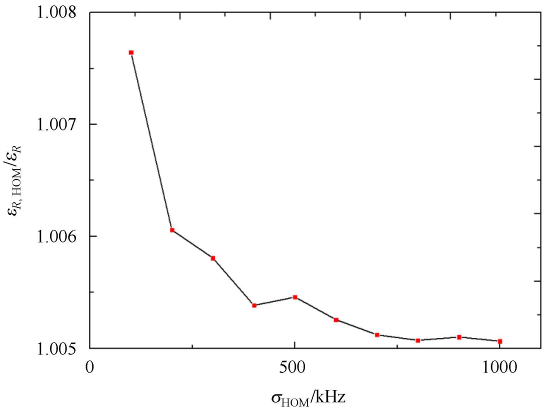

Fig. 11. Multi-bunch emittance increase against RMS frequency spread width for the dipole modes sitting on machine line.

3.4 Conclusion and discussion

The beam instability induced by the transverse parasitic modes in the β=0.63 and β=0.82 sections of the ADS driver linac in China has been studied in detail.

Multi-bunch effective emittance ε_R is introduced to more reasonably evaluate the dipole mode induced instability. $\varepsilon_{R,\mathrm{HOM}}/\varepsilon_R<1.4$ is then used as the tolerable limit of the multi-bunch effective emittance increase.

In reality, the single bunch emittance ε_0 may be higher than 0.26 πmm·mrad because it is basically impossible to include all kinds of jitters and errors in the machine dynamics design stage, for this scenario $\varepsilon_{R,\mathrm{HOM}}$ and ε_R will go to higher values than the case of ε_0=0.26 πmm·mrad, while the calculated emittance increase $\varepsilon_{R,\mathrm{HOM}}/\varepsilon_R$ will go to a lower one. Although the tolerable limit will also go to a lower value as ε_0 increases, the final conclusion of this paper will not go to the opposite side. Fig. 12 shows the dependence of $\varepsilon_{R,\mathrm{HOM}}/\varepsilon_R$ and the tolerable limit on the single bunch emittance ε_0, which indicates that the emittance increase caused by dipole modes is always lower than the tolerable limit when ε_0 is increased from 0.26 πmm·mrad to 2.6 πmm·mrad at the safety margin current of 100 mA.

By varying the damping Q_{ext}, the emittance increase is calculated for the beam current ranging from 10 mA to 100 mA. It is found that the multi-bunch effective emittance increase is lower than the tolerable limit even for Q_{ext}=10^8 and I_{b}=100 mA. The dipole modes can also be excited by the cavity misalignment and the off-axis injected beam, both of which will strengthen the dipole mode effect only induced by the beam input jitters. However, the strengthening effect is fairly low. In addition, the effect of the dipole mode sitting on the machine line is also investigated, which shows that it is not a concern either.

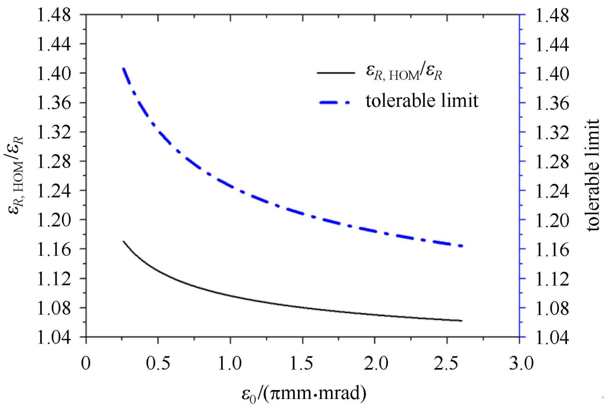

Fig. 12. $\varepsilon_{R,\mathrm{HOM}}/\varepsilon_R$ and the tolerable limit against ε_0 at the safety margin current of 100 mA.

Based on the studies conducted in this paper, HOM couplers are not required for the nominal operation of the ADS driver linac. However, in order to facilitate the beam transport line design downstream of the linac, it is recommended that HOM couplers are installed, which would also be beneficial for the future flexibility of the machine operation.

The authors would like to thank all the colleagues in the ADS beam dynamics group for helpful discussions and Marcel Schuh for his generous offer of the SMD code.

References

1 TANG Jing-Yu, LI Zhi-Hui et al. Conceptual Physics Design on the C-ADS Accelerators. IHEP-CADS-Report/2011-1E, IHEP & IMP, 2012.8
2 CHENG Peng, PEI Shi-Lun, WANG Jiu-Qing et al. Effects of Longitudinal Parasitic Modes on the Beam Dynamics for the ADS Driving Linac in China. Chin. Phys. C (HEP&NP), to be published
3 Simulate higher order Mode Dynamics (SMD) code repository. https://svnweb.cern.ch/trac/splhombbu
4 Panofsky W K H, Wenzel W A. Review of Scientific Instruments, 1956, **27**(11): 967
5 Marcel S. Study of Higher Order Modes in Superconducting Accelerating Structures in Linac Applications (Ph.D. Thesis). CERN, 2011
6 http://irfu.cea.fr/Sacm/logiciels/index3.php
7 Ainsworth R, Molloy S. Nuclear Instruments and Methods in Physics Research A, 2014, **734**: 95–100
8 Jeon D, Merminga L, Krafft G. Nuclear Instruments and Methods in Physics Research A, 2002, **495**: 85–94
9 Computer Simulation Technology (CST), 2010.10. www.cst.com